X-621-68-397
PREPRINT

A NEUTRAL PARTICLE WAKE EXPERIMENT FOR MEASURING UPPER ATMOSPHERE TEMPERATURES FROM A MOVING VEHICLE

I. BRACE
C. WU

NOVEMBER 1968

GSFC — GODDARD SPACE FLIGHT CENTER
GREENBELT, MARYLAND

CONTENTS

A NEUTRAL PARTICLE WAKE EXPERIMENT FOR MEASURING UPPER ATMOSPHERE TEMPERATURES FROM A MOVING VEHICLE

L. H. Brace and W. C. Wu

ABSTRACT

A method is discussed for measuring the kinetic temperature of the neutral particles in the upper atmosphere. A suitable baffle is mounted an appropriate distance in front of the orifice of a satellite-borne neutral particle mass spectrometer. As the satellite spins, the neutral particle wake formed by the baffle scans across the orifice and causes a bite-out of the pressure maximum which would otherwise be observed by the spectrometer as the orifice rotates through the velocity vector. At very low temperatures the baffle would completely block the orifice from the stream of thermal particles through which the satellite is moving, and the pressure in the spectrometer would be reduced to zero as the orifice passed through zero angle of attack. At atmospheric temperatures (500-2000°K), a suitable baffle produces a pressure reduction which varies approximately inversely with the temperature.

Since the various neutral particle species have different thermal velocities, each will independently produce its own wake. The baffle performs a kind of mass discrimination in which the lateral components of thermal motion cause the lighter species to form the near-wake and the heavier species to form a more extended wake. Thus, at any given distance behind the baffle, a greater pressure reduction is observed for the heavier species.

When chemically active species such as atomic oxygen are sampled the depth of modulation will still reflect the temperature, but the absolute amplitudes of the pressure inside the chamber will depend upon the amount of recombination. When mixtures of atomic and molecular species are present in the atmosphere, this technique provides an additional source of information regarding the relative concentrations of the atomic and molecular species.

A NEUTRAL PARTICLE WAKE EXPERIMENT FOR MEASURING UPPER ATMOSPHERE TEMPERATURES FROM A MOVING VEHICLE

INTRODUCTION

The gas kinetic temperature (T_0) is a parameter of considerable interest in the physics of the upper atmosphere. Nearly all of our knowledge about its behavior has been inferred from neutral particle scale heights based on satellite drag studies (Jacchia, 1964). Direct measurements from satellites have not generally lead to entirely reliable neutral particle scale heights because of latitudinal and local time structure which is superposed upon the changes of neutral density with altitude. Therefore, reliable measurements of gas temperature have been limited to a few rocket flights in which true vertical profiles of individual species have been measured (Spencer et al, 1965) (Nier, et al, 1964).

The major difficulty encountered in measuring T_0 directly from a satellite, or a rocket, is that the translational velocity of the measuring platform greatly exceeds the thermal velocity of the particles. Therefore the flux of particles flowing to a sensor experiences extremely wide variation with angle of attack. At satellite velocities, these variations are relatively insensitive to T_0. The method discussed here overcomes this difficulty by interrupting the directed stream by means of a rectangular baffle. The method is very sensitive to T_0 because the particles which populate the wake of the baffle do so only because of their thermal motion. It will be shown that the amplitude of the pressure in the wake, or conversely the depth of pressure reduction in the wake, is a strong function of the kinetic temperature.

DESCRIPTION OF THE EXPERIMENT

If the measurement is to be performed on a spinning satellite, as we have thus far assumed, a long rectangular baffle is mounted at a distance of several inches in front of a small orifice leading to the ionization chamber of a neutral particle mass spectrometer. This arrangement is mounted perpendicular to the spin axis of the spacecraft as shown in figure 1. As the satellite spins, the neutral particle wake which forms behind the baffle scans across the orifice and reduces the flux of neutrals into the chamber. This causes a reduction of the partial pressure of each species as the angle of attack passes through zero. At the limit of zero temperature, the baffle would completely block the orifice from the stream of particles through which the satellite was moving, and no

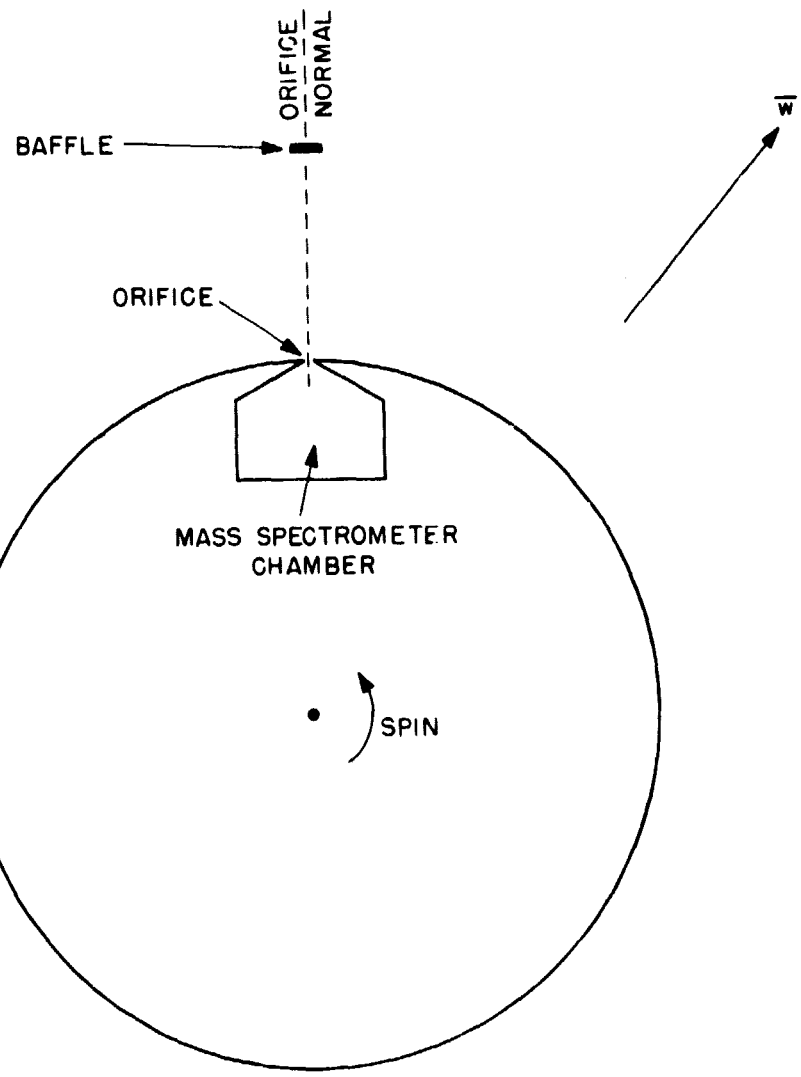

Figure 1–Experimental arrangement. As the satellite spins, the long rectangular baffle (seen from the narrow dimension) passes between the velocity vector, $\bar{w}$, and the orifice. The wake which forms behind the baffle scans across the orifice and causes a pressure reduction which depends upon the thermal velocity of the particles sampled.

thermal particles could enter the orifice. However, at the high temperatures found in the upper atmosphere, the reduction in pressure behind the baffle is much less because the thermal motion of the particles causes them to fill-in behind the baffle more rapidly. This effect is illustrated in figure 2 which shows the relative sizes of the wake for H, H_e, O and N_2 behind a very large baffle. In constructing this drawing we have assumed that the thermal velocity of H is comparable to the satellite velocity. Clearly the depth of the pressure well in the wake increases with the mass of the particle. The depths of the "pressure wells" for a fixed translational velocity depend upon the choice of R/ℓ, the prime variable in designing the experiment.

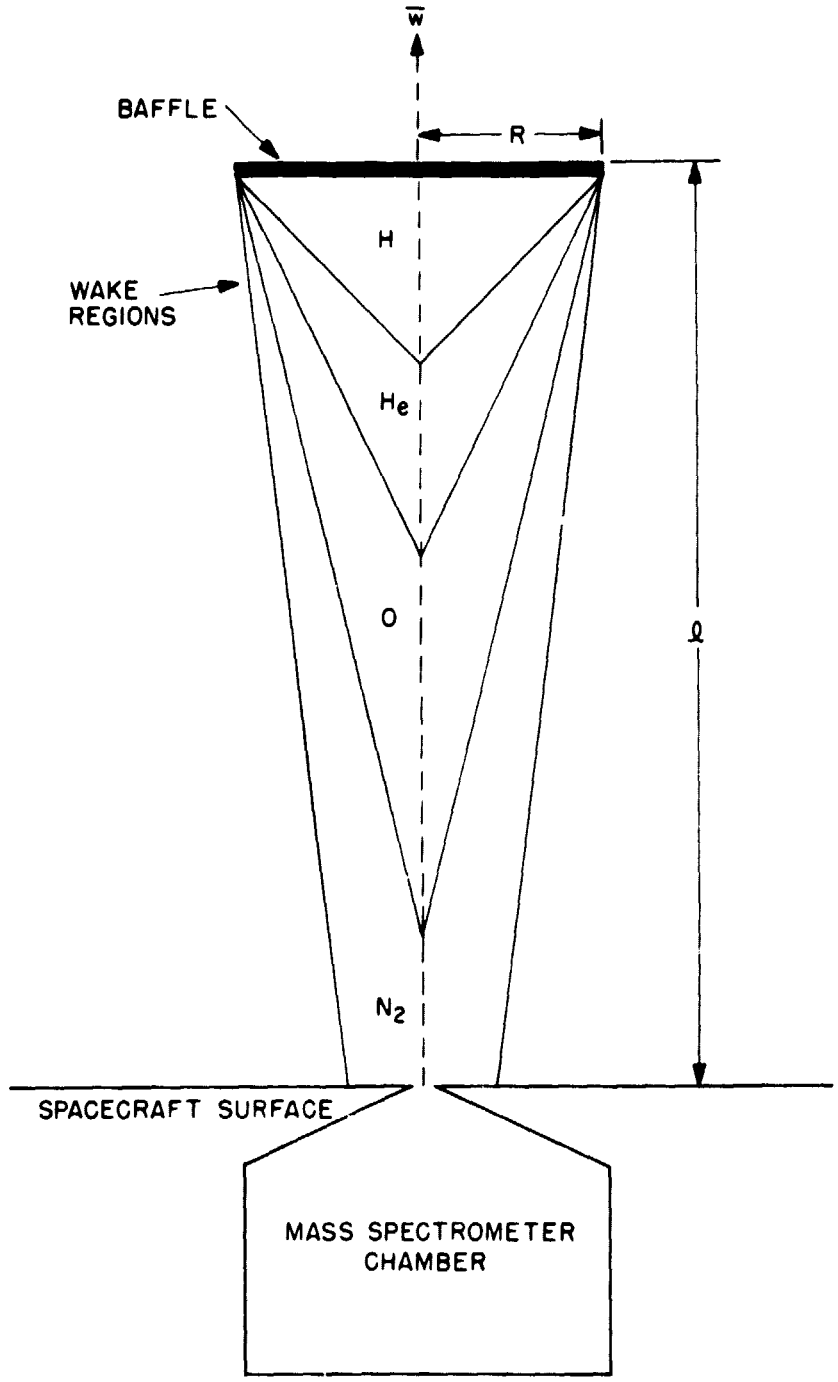

Figure 2–Relative sizes of the wake for various neutral species, assuming the velocity of the satellite is comparable to the thermal velocity of atomic hydrogen. The wake boundaries are arbitrarily defined.

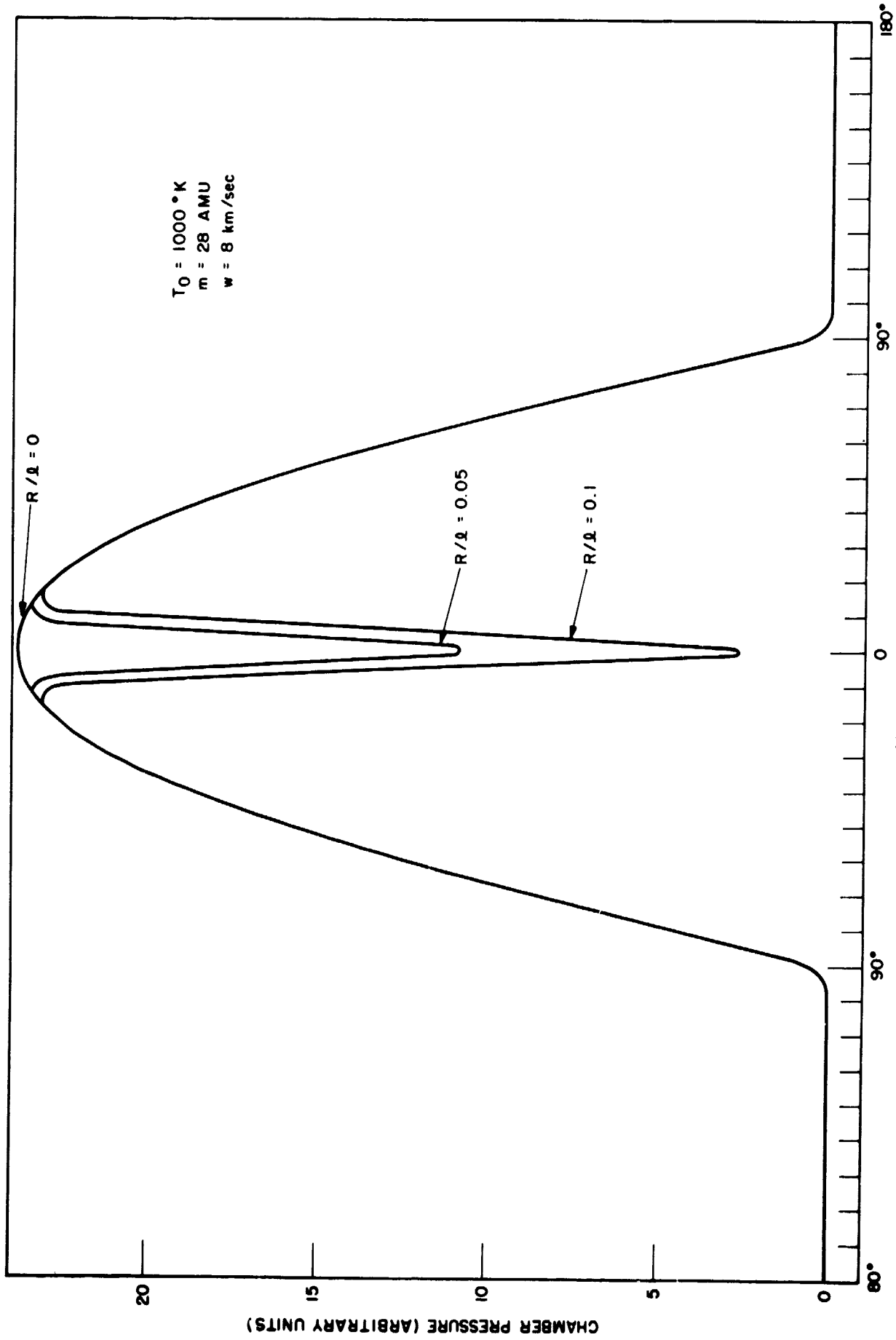

Figure 3–Chamber Pressure of N_2 as a function of angle of attack, for $R/\ell = 0$, 0.05 and 0.1.

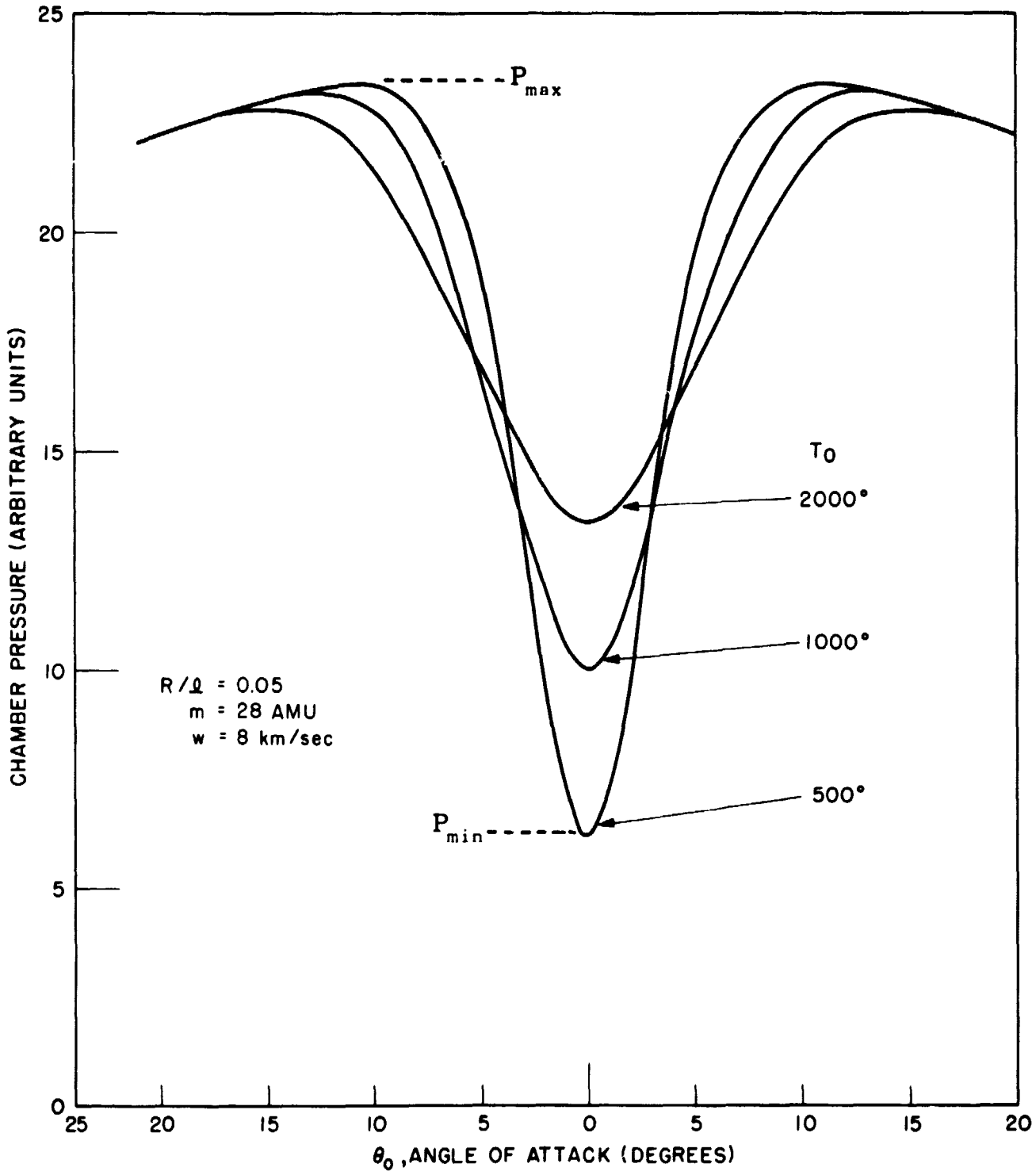

Figure 4—The effect of atmospheric temperature upon the pressure well for a baffle $R/\ell = 0.05$. The temperature affects both the depth and width of the pressure trough.

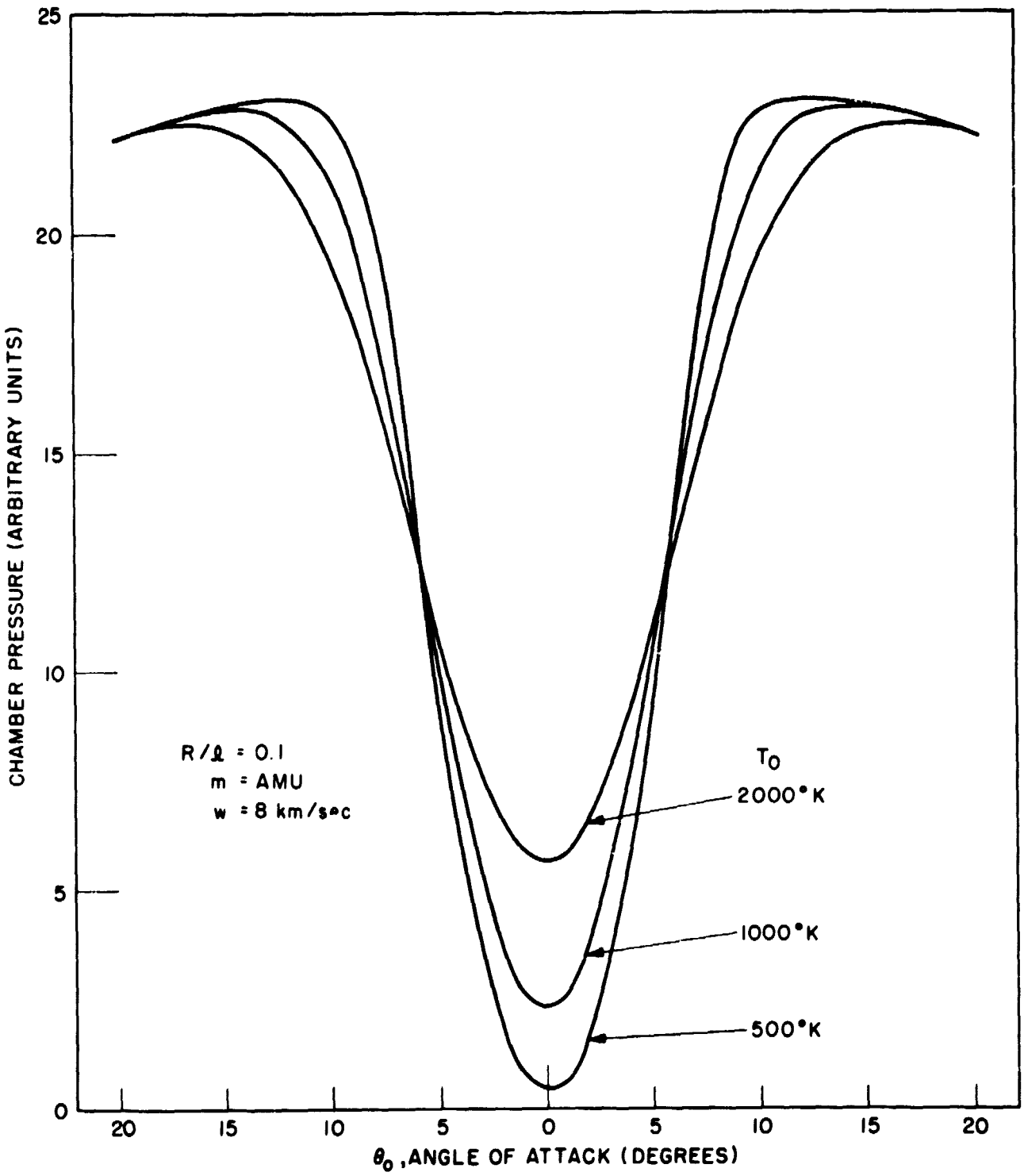

Figure 5–The effect of atmospheric temperature upon the pressure well for a baffle $R/\ell = 0.1$.

scale is expanded about zero to show only the portion of the pressure characteristic which is affected by the baffle. Nearly the entire range of exospheric temperature is encompassed by the three curves shown (500°, 1000°, 2000°).

The atmospheric temperature modifies both the depth and the width of the pressure well. The pressure reduction ratio P_{min}/P_{max}, is 0.60 for 2000°K and 0.265 for 500°K when the 0.05 baffle is used. When the 0.1 baffle is used, the pressure reduction ratio is 0.25 for 2000°K and 0.022 for 500°K. From this it can be seen that, in theory, the larger baffles provide greater resolution in the temperature. In practice, however, the minimum pressure which can be resolved depends upon experimental factors such as the background pressure due to contaminants, the gas time constant of the orifice-chamber system, the sensitivity of the spectrometer and the telemetry resolution.

Although the background pressure can be measured during each spin cycle as the orifice looks back into the spacecraft wake, the background itself may be orientation dependent, or time dependent.

The gas time constant of the system can be made adequate by maintaining a large ratio of orifice area to chamber volume as well as by selecting a suitably low spin rate. Spin rates of as great as 20 rpm should be possible. The effects of the orifice radius upon the pressure characteristics are second order, as discussed in Appendix B. Therefore the gas time constant can be accommodated.

The sensitivity of the spectrometer ultimately limits the altitude to which a given species can be employed for the neutral wake measurements. The most abundant species are the most desirable in this regard, therefore N_2 and O are the prime constituents to be employed in the Earth's atmosphere.

The telemetry systems currently in use provide telemetry accuracy of about 1/2% of full scale. Although current detection schemes could be devised for increased electronic resolution of the pressure well (P_{min}), the telemetry accuracy will ultimately limit the depth of the pressure well which could be resolved.

For the reasons given above the R/ℓ should be selected to produce perhaps less than a factor of ten reduction in the partial pressure of the species of prime interest.

The Pressure Curves for Other Particle Masses

Although all of the calculations represented in figures 3, 4 and 5 were carried out for N_2, some feeling for the effect of employing other species can be obtained from these figures because the thermal velocity (c_m) depends upon both the temperature and mass of the particle.

$$c_m = (2kT_0/m)^{1/2}$$

Thus a factor of four increase in T_0 is equivalent to a factor of four decrease in m. For example, in a theoretical sense, the curves in figures 4 and 5 labelled 500°, 1000° and 2000°K could equally well have been labelled masses 28, 14 and 7, at a fixed temperature of 500°K.

The Measurement of Atomic Species

Atomic constituents such as O can also be employed for determining the temperature. At most satellite altitudes (>250 km), nearly all of the oxygen exists in atomic form. Although the influx of O into the orifice will be described properly by the theory, the flow of O out of the orifice (equation 8) will be reduced by the amount of recombination occurring on the walls of the chamber. As a result, the amplitude of the partial pressure curves for O will be less than would otherwise be expected. However, the relative shape of the O curves is not necessarily changed by surface recombination unless the percentage recombination is pressure-dependent. It seems reasonable to assume that the recombination factor would be constant as long as the mean free path is much greater than the chamber dimensions. In this case, the flux of O into the chamber (G_i) is balanced by the out flux (G_0) and the recombination flux (αG_i).

$$G_i = G_0 + \alpha G_i$$

or

$$G_0 = G_i (1 - \alpha)$$

where α is the fraction of incoming particles which recombine before leaving. If α is constant as we have assumed, then the recombination flux will simply change the ratio of the incoming and outgoing O flux. This will reduce the absolute amplitude of O pressure but will not change its relative pressure modulation. Since the temperature is derived from the latter, it should be feasible to employ the atomic oxygen data for the measurement of temperature. This is important because atomic oxygen is the major constituent at the altitudes where this technique would be applied.

From the above discussion it is apparent that any attempt to determine the absolute concentration of atomic constituents requires that the molecular form

also be measured so that the recombination losses can be evaluated. If the only source of O_2 is the recombined O, then both the O and O_2 pressure characteristics carry the same temperature information. Thus the temperature can be obtained from either without prior evaluation of the recombination fraction, if this fraction is independent of the chamber pressure.

Mixtures of Atomic and Molecular Species

If the neutral wake method were employed at lower altitudes where both O and O_2 are abundant, (as would be encountered below 200 kilometers on rockets or low perigee satellites) the arguments of the previous paragraphs could be inverted to determine the relative concentrations of atomic and molecular oxygen in the atmospheric sample. In this case, the temperature would be derived from the N_2 (or O) pressure characteristics. The pressure modulation in O would still reflect only the gas temperature, but the O_2 pressure characteristics would now have two components (1) the internally recombined oxygen having the same shape as the O characteristics, and (2) the atmospheric O_2 having a much greater depth of modulation corresponding to its greater mass. Thus the relative concentrations of O and O_2 in the atmosphere control the relative depth of the pressure well observed in O_2. In practice the relative concentrations of O and O_2 would be derived by adjusting their values to reproduce the observed O_2 pressure well theoretically.

Tne Effects of Particle Backscattering

A potential source of error in the neutral wake method arises from the double scattering of particles from the satellite surface to the back of the baffle and then into the orifice. This effect must be rather small at small angles of attack for the following reasons. The same flux of particles which is occulted by the front of the baffle also impacts the entire forward surface of the spacecraft. An equivalent flux is therefore flowing away from the satellite, and some of this impacts the inward side of the baffle. Fortunately little of the flux which is re-emitted by the baffle actually reaches the orifice because of the small solid angle it subtends when viewed from the baffle. In any event, the random flux scattered into the orifice will be extremely small compared to the directed stream which the baffle intercepts.

If a given application requires further reduction of the backscattered component, one could shape the inside surface of the baffle to direct the scattered particles away from the orifice. The entire experiment might also be mounted on a boom to reduce the amount of surrounding area for the initial backscattering.

Some effects of backscattering should be evident at angles of attack beyond 90° where the orifice is looking into the spacecraft wake but the inside of the baffle is still receiving the full stream, as shown in figure 6. If these fluxes produce detectable pressure, they may be valuable for estimating the amount of backscattering occurring at zero angle of attack.

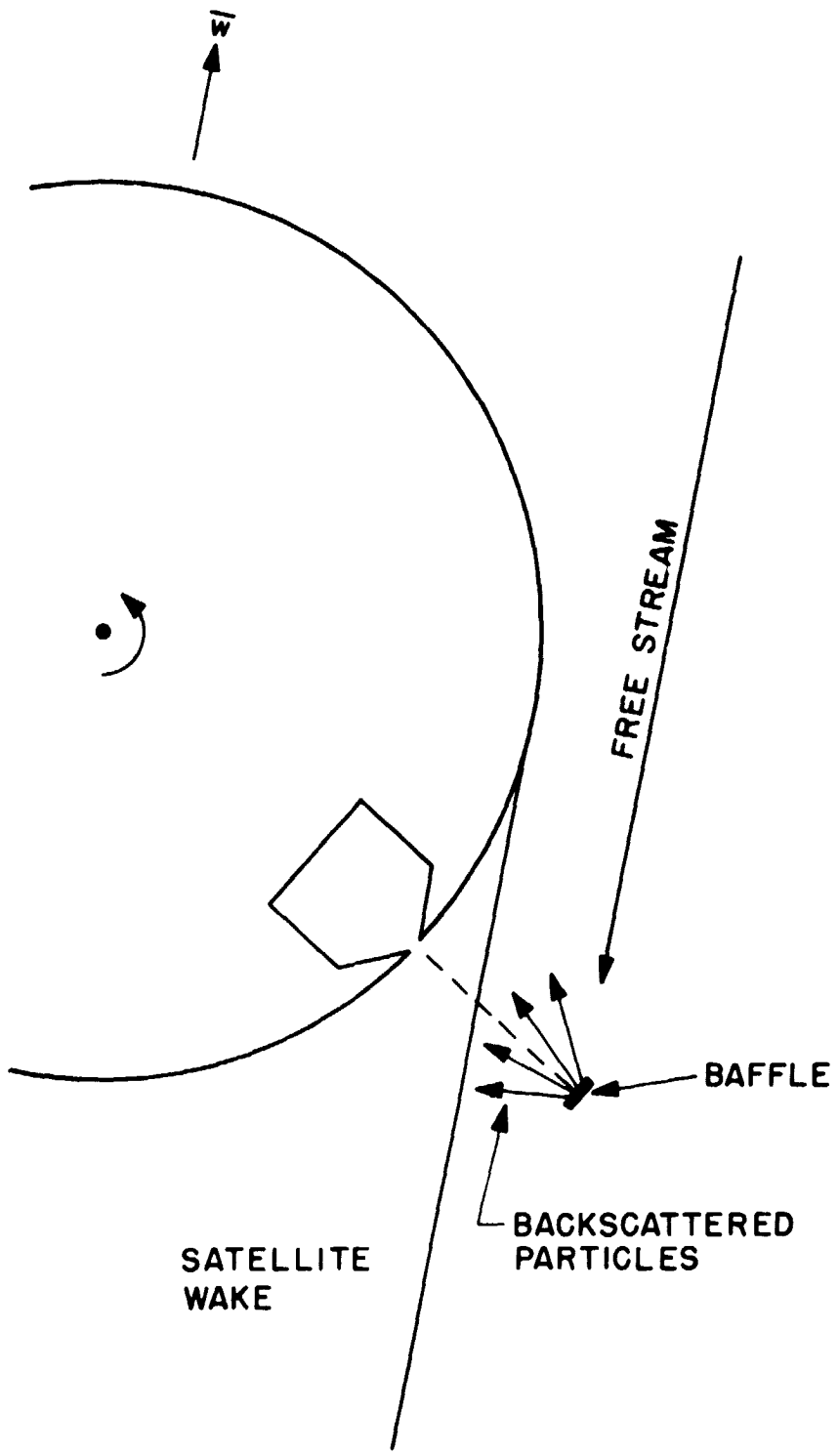

Figure 6–A situation in which backscattered particles could be observed in the absence of the direct stream.

In the case of atomic species, the back of the baffle and the surrounding area might be treated to enhance the surface recombination, thus minimizing the amount of the atomic form which would reach the orifice through backscattering.

SUMMARY

In summary, it appears feasible to employ the wake behind a moving baffle to investigate the thermal velocities of various neutral particle constituents of the upper atmosphere. If the partial pressures of the various species are resolved by a neutral particle mass spectrometer, the temperature of the atmosphere can be derived independently from more than one species. When both atomic and molecular forms of a gaseous element are present in the region, the depth of the wake provides additional information on their relative abundances.

We have demonstrated the effects of the following factors: (1) Baffle size and mounting distances, (2) atmospheric temperature and mass, and (3) orifice size (Appendix B). The effect of particle scattering has been estimated to be small.

ACKNOWLEDGEMENTS

The authors are indebted to Raymond A. Sears for his aid in writing the computer programs for the numerical solutions. We also thank George Carignan, and Paul Hays from the University of Michigan, James C. G. Walker from Yale University and David Pelz and George Newton of Goddard Spaceflight Center for valuable discussions regarding the feasibility of the technique.

REFERENCES

Jacchia, L. G., "The Temperature above the thermopause," Smithsonian Astrophysical Observ. Rept. 150, April 22, 1964.

Nier, A. O., J. H. Hoffman, C. Y. Johnson, and J. C. Holmes, "Neutral composition of the atmosphere in the 100 to 200 kilometer range," J. Geophys. Res., 69, 979-989, 1964.

Spencer, N. W., L. H. Brace, G. R. Carignan, D. R. Taeusch, H. Niemann, "Electron and molecular nitrogen temperature and density in the thermosphere," J. Geophys. Res., 70, 2665-98, 1965.

Schultz, F. V., N. W. Spencer, and A. Reifman, "Atmospheric pressure and temperature measurements between the altitudes of 40 and 110 kilometers," Univ. of Michigan Eng. Res. Inst., Rept. 2, Ann Arbor, July 1948.

APPENDIX A
Theory of the Neutral Particle Wake Experiment

List of Symbols

T_0 = gas kinetic temperature of the atmosphere outside

T_i = gas kinetic temperature in the chamber

k = Boltzmann constant

n_0 = gas concentration in the atmosphere outside

n_i = gas concentration in the chamber

m = mass of the gas particle

P_0 = gas pressure in the atmosphere outside

P_i = gas pressure in the chamber

$\bar{v}$ = thermal velocity of the gas particle

$\bar{w}$ = translational velocity of the instrument

R = half width of the baffle

ℓ = distance between the orifice and the baffle

f_s = velocity distribution function of particles

f = velocity distribution function of particles relative to a moving sensor

r = radius of the orifice

In this appendix, we outline the procedure for calculating the pressure modulation caused by a baffle which is mounted in front of an orificed chamber on a spinning satellite, as described in the preceding paper. First we develop the integral equations describing the flux of particles into and out of the orifice without a baffle. By equating these flows and employing the gas law, we arrive at an integral equation describing the ratio of internal pressure to atmospheric pressure, P_i/P_0. We outline the method of numerical solution of this equation. We then introduce the baffle by suitably modifying one of the integration limits on the angle of attack integral.

The Theoretical Development

The neutral particles in the atmosphere are assumed to obey the Maxwell-Boltzmann velocity distribution,

$$f_s(\bar{v}) = n_0 \left(\frac{m}{2\pi k T_0}\right)^{3/2} e^{-\frac{m}{2kT_0}(\bar{v})^2} \tag{1}$$

The velocity distribution relative to a sensor system moving with velocity $\bar{w}$ becomes

$$f(\bar{v}) = n_0 \left(\frac{m}{2\pi k T_0}\right)^{3/2} e^{-\frac{m}{2kT_0}(\bar{v}+\bar{w})^2}. \tag{2}$$

We select our coordinate system in such a way that the z-axis is the orifice normal and the velocity vector, $\bar{w}$, lies in the x-z plane, as shown in figure 7. Using vector notation,

$$\bar{w} = (w \sin\theta_0, 0, w\cos\theta_0). \tag{3}$$

The flux density of atmospheric particles reaching the orifice (the origin) can be expressed

$$G_i = \int_{\varphi=0}^{2\pi}\int_{\theta=0}^{\pi/2}\int_{v=0}^{\infty} n_0\left(\frac{m}{2\pi k T_0}\right)^{3/2} e^{-\frac{m}{2kT_0}(\bar{v}+\bar{w})^2} v\cos\theta\, d\varphi\, d(-\cos\theta) v^2 dv. \tag{4}$$

The range of thermal velocities which can flow into the orifice can be expressed

$$\bar{v} = (-v\sin\theta\cos\varphi, -v\sin\theta\sin\varphi, -v\cos\theta). \tag{5}$$

After the particles enter the chamber, they become thermalized by multiple collisions. The flux density of particles which flow out of the orifice is then given by

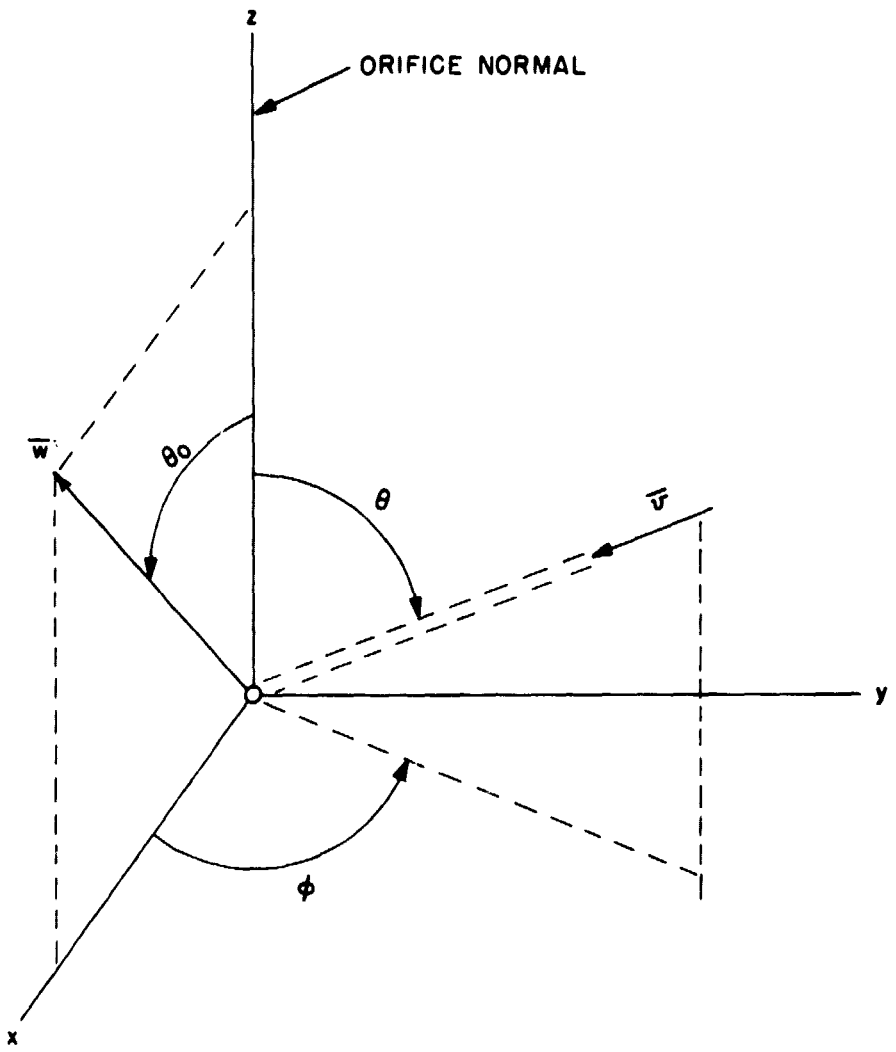

Figure 7–The coordinate system employed in the theory. The velocity vector, $\bar{w}$, always remains in the x-z plane and the angle of attack, θ_0, is the angle between the orifice normal (z-axis) and $\bar{w}$.

$$G_0 = \int d^3\bar{v}\, f_s(v)\, v \cos\theta \tag{6}$$

which can be shown to be

$$G_0 = \int_{\varphi=0}^{2\pi} \int_{\theta=0}^{\pi/2} \int_{v=0}^{\infty} n_i \left(\frac{m}{2\pi k T_i}\right)^{3/2} e^{-\frac{m v^2}{2kT_i}}\, v \cos\theta\, d\varphi\, d(-\cos\theta)\, v^2\, dv \tag{7}$$

$$= n_i\, k\, T_i / (2\pi m k T_i)^{1/2} . \tag{8}$$

Assuming no source or sink of particles within the chamber, the in flow and the outflow will be identical

$$G_0 = G_i \quad . \tag{9}$$

By invoking the kinetic gas law

$$P_i = n_i \, k \, T_i$$
$$P_0 = n_0 \, k \, T_0 \tag{10}$$

and combining (4), (5) and (7), the pressure ratio between the chamber and the atmosphere is found to be

$$\frac{P_i}{P_0} = \left(\frac{T_i}{T_0}\right)^{1/2} \frac{1}{\pi} \int_{\varphi=0}^{2\pi} \int_{\theta=0}^{\pi/2} \left[(s_1^2 + 1) e^{-(w/c_m)^2} + \pi^{1/2} s_1 (1.5 + s_1)(1 + \operatorname{erf} s_1) \right. \tag{11}$$
$$\left. e^{-(w/c_m)^2} e^{s_1^2} \right] \sin\theta \cos\theta \, d\theta \, d\varphi$$

where

$$s_1 = \frac{w}{c_m} [\sin\theta_0 \sin\theta \cos\varphi + \cos\theta_0 \cos\theta] \tag{12}$$

$$c_m = (2kT_0/m)^{1/2}, \text{ the most probable velocity} . \tag{13}$$

Equation (11) is equivalent to a simpler formula

$$\frac{P_i}{P_0} = \left(\frac{T_i}{T_0}\right)^{1/2} [e^{-s^2} + s\pi^{1/2}(1 + \operatorname{erf} s)] \tag{14}$$

where

$$s = \frac{w}{c_m} \cos\theta_0$$

developed by Schultz, et al, 1948. However, the integral form (11) permits geometrical structure which may be in view of the orifice to be considered. The difference (11) and (14) arises from the technique of integration.

The Numerical Integration Method

The numerical integration is carried out by computer in the following manner. Writing (11) in the form

$$\frac{P_i}{P_0} = \left(\frac{T_i}{T_0}\right)^{1/2} \frac{1}{\pi} \int_{\varphi=0}^{2\pi} \int_{\theta=0}^{\pi/2} F(\theta, \varphi)\, d\theta\, d\varphi \tag{15}$$

where

$$F(\theta, \varphi) = \left[(s_1^2 + 1)\, e^{-\left(\frac{w}{c_m}\right)^2} + \pi^{1/2} s_1 (1.5 + s_1)^2 (1 + \operatorname{erf} s_1) e^{-\left(\frac{w}{c_m}\right)^2 + s_1^2} \right] \tag{16}$$

θ is divided into 180 intervals

$$\left(0, \frac{\pi}{360}, \frac{2\pi}{360}, \ldots \frac{\pi}{2}\right)$$

and the resulting 181 points are named

$$(1, 2, 3, \ldots 181).$$

φ is divided into 360 intervals

$$\left(0, \frac{\pi}{360}, \frac{\pi}{360} \ldots 2\pi\right)$$

and the resulting points are named

$$(1, 2, 3, \ldots 361).$$

The numerical integration is carried out as indicated

$$\frac{P_i}{P_0} = \left(\frac{T_i}{T_0}\right)^{1/2} \frac{1}{\pi} \int_{\varphi=0}^{2\pi} \sum_{i=1}^{180} [F(\theta_i, \varphi) + F(\theta_{i+1}, \varphi)] \frac{\pi}{360} \, d\varphi . \qquad (17)$$

Letting

$$g(\varphi) = \sum_{i=1}^{360} [F(\theta_i, \varphi) + F(\theta_{i+1}, \varphi)] \frac{\pi}{360},$$

$$\frac{P_i}{P_0} = \left(\frac{T_i}{T_0}\right)^{1/2} \frac{1}{\pi} \sum_{i=1}^{360} [g(\varphi_i) + g(\varphi_{i+1})] \frac{\pi}{360}, \qquad (18)$$

$$= H(T_i, T_0, w, c_m, \theta_0) \qquad (19)$$

In test cases, the numerical calculations by computer agrees with the earlier form of the pressure equation (14) within 0.1%.

Introducing the Baffle

If the baffle takes the form of a long rectangular strip, as shown in figure 8, the integration limit on θ in equation 11 must be modified. The trigonometric relationship of the angles shown in the figure are

$$\text{Tan } \theta_c = \frac{Q}{\ell}$$

$$\text{Cos } \varphi = \frac{R}{Q} \qquad (20)$$

$$\therefore \theta_c = \text{Tan}^{-1} \frac{Q}{\ell} = \text{Tan}^{-1} \left| \frac{R}{\ell} \quad \frac{1}{\cos \varphi} \right| = \sin^{-1} \frac{R}{[R^2 + (\ell \cos \varphi)^2]^{1/2}}$$

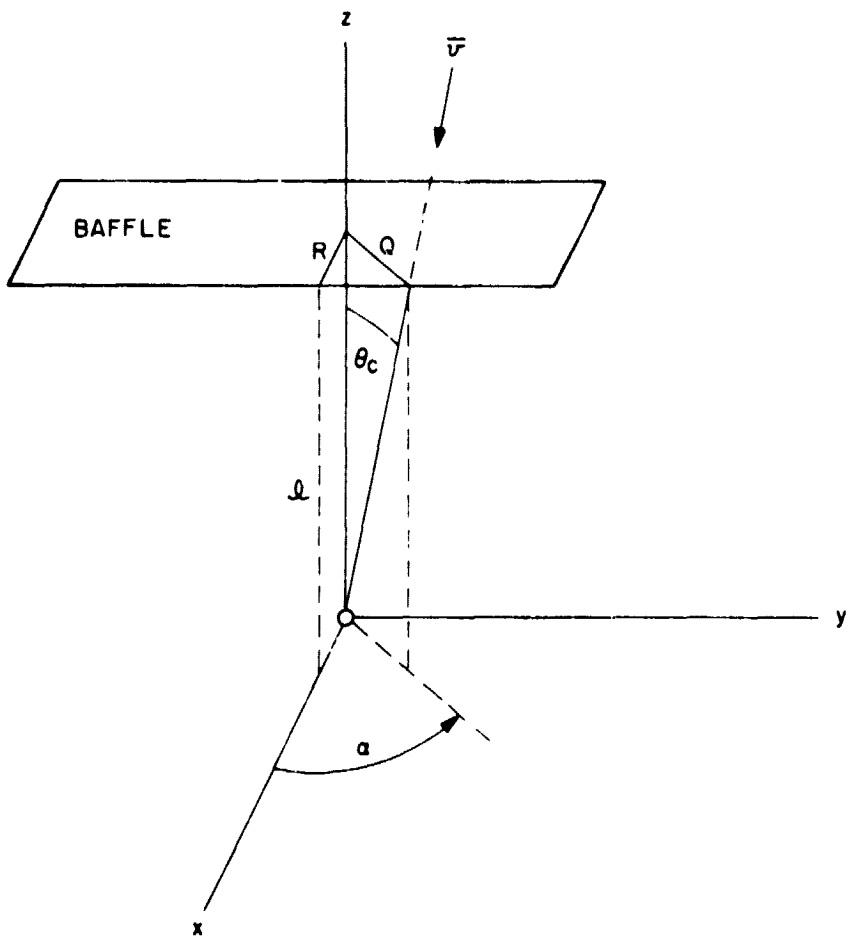

Figure 8–The baffle coordinate system.

where θ_c is the critical angle below which a particle arriving from azimuth angle φ will have no chance of reaching the origin (the orifice). The selection of baffle half width, R, and distance, ℓ, thus controls this critical angle which becomes the lower integration limit on θ, as shown in equation (21),

$$\frac{P_i}{P_0} = \left(\frac{T_i}{T_0}\right)^{1/2} \frac{1}{\pi} \int_{\varphi=0}^{2\pi} \int_{\theta_c}^{\pi/2} F(\theta, \varphi)\, d\theta\, d\varphi . \qquad (21)$$

The numerical integration process described earlier was employed to solve (21) for the several baffle dimensions and atmospheric temperatures represented by figures 3, 4 and 5.

APPENDIX B
Consideration of Orifice Size

In the calculations carried out thus far, we have assumed that the orifice was very small compared to the dimensions of the baffle and therefore the dimensions of the wake. For orifice sizes usually employed, this assumption is reasonably valid. However, there may be a variety of reasons for desiring a larger orifice on any particular flight. For example, if the spin rate is high and the chamber is large, a larger orifice area may be necessary to maintain steady state flow into and out of the chamber. For this reason we have calculated the effect of the orifice size upon the pressure modulation.

We divided the orifice into seven strips running parallel to the occulting baffle, as shown in figure 9. We calculated P_i/P_0 for each strip and found the average P_i/P_0 by multiplying by an area factor.

$$\bar{P}_i/P_0 = \sum_{j=1}^{7} (P_i \; P_0)_j \; A_j \; . \tag{22}$$

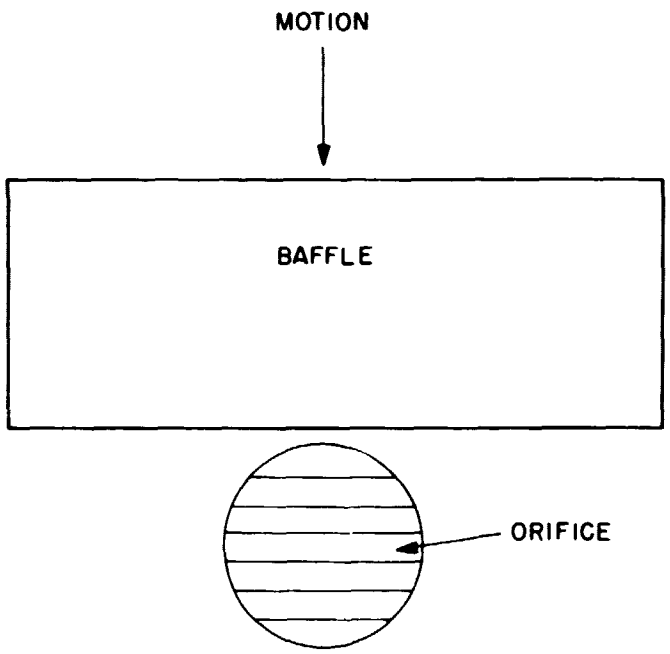

Figure 9–The effect of the baffle occulting a finite size baffle.

For each strip, the integration limit θ_c is given by

$$\theta_c = \sin^{-1} \frac{R \pm C_j r}{[(R \pm C_j r)^2 + (\ell \cos \varphi)^2]^{1/2}} \qquad (23)$$

where

$R + C_j r$ when $0 < \varphi < 180°$

$R - C_j r$ $\qquad 180 < \varphi < 360°$

C_j = constant determined by geometric relationship

r = orifice radius.

To illustrate the effect of finite orifice sizes, figures 10 and 11 show N_2 pressure curves for $R/\ell = 0.05$ and 0.1, respectively, and for orifice radii of 0, 0.2 and 0.5 inches. From equation 23 it is clear that the actual sizes of R and ℓ are important for this effect, rather than just the value of R/ℓ. We assumed a baffle distance of 10 inches and a half width of one inch and one half inch, respectively.

From the figures it is apparent that the orifice radius does not significantly affect the depth of the pressure well until the radius approaches 1/2 inch. This can be understood qualitatively from figure 9 by considering the projection of the baffle as it occults the orifice. The initial occultation affects little of the total area, so the pressure reduction is not changed much. Thus the fluxes through the inner slices tend to dominate the shape of the pressure well.

From this viewpoint, alternate orifice shapes might be considered. For example, it is apparent that only the orifice dimensions perpendicular to the baffle scan direction can cause important modification of the pressure characteristic. Therefore one might employ a long rectangular orifice parallel to the baffle to obtain a large gas conductance without reducing the depth of the pressure well.

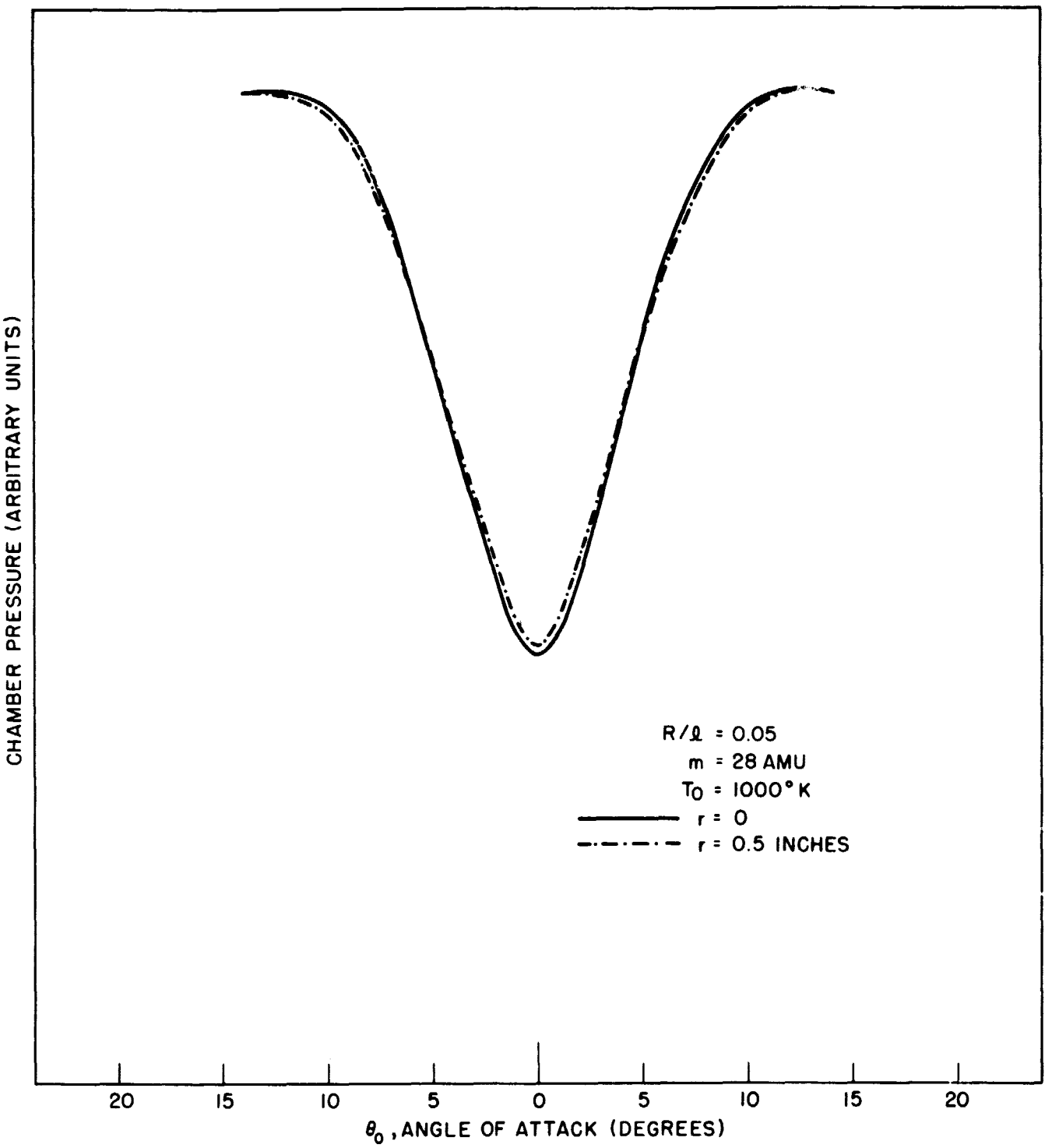

Figure 10–The effect of a finite size orifice (radius 0.5 inch) upon the pressure well for $R/\ell = 0.05$ and employing N_2 at 1000°K.

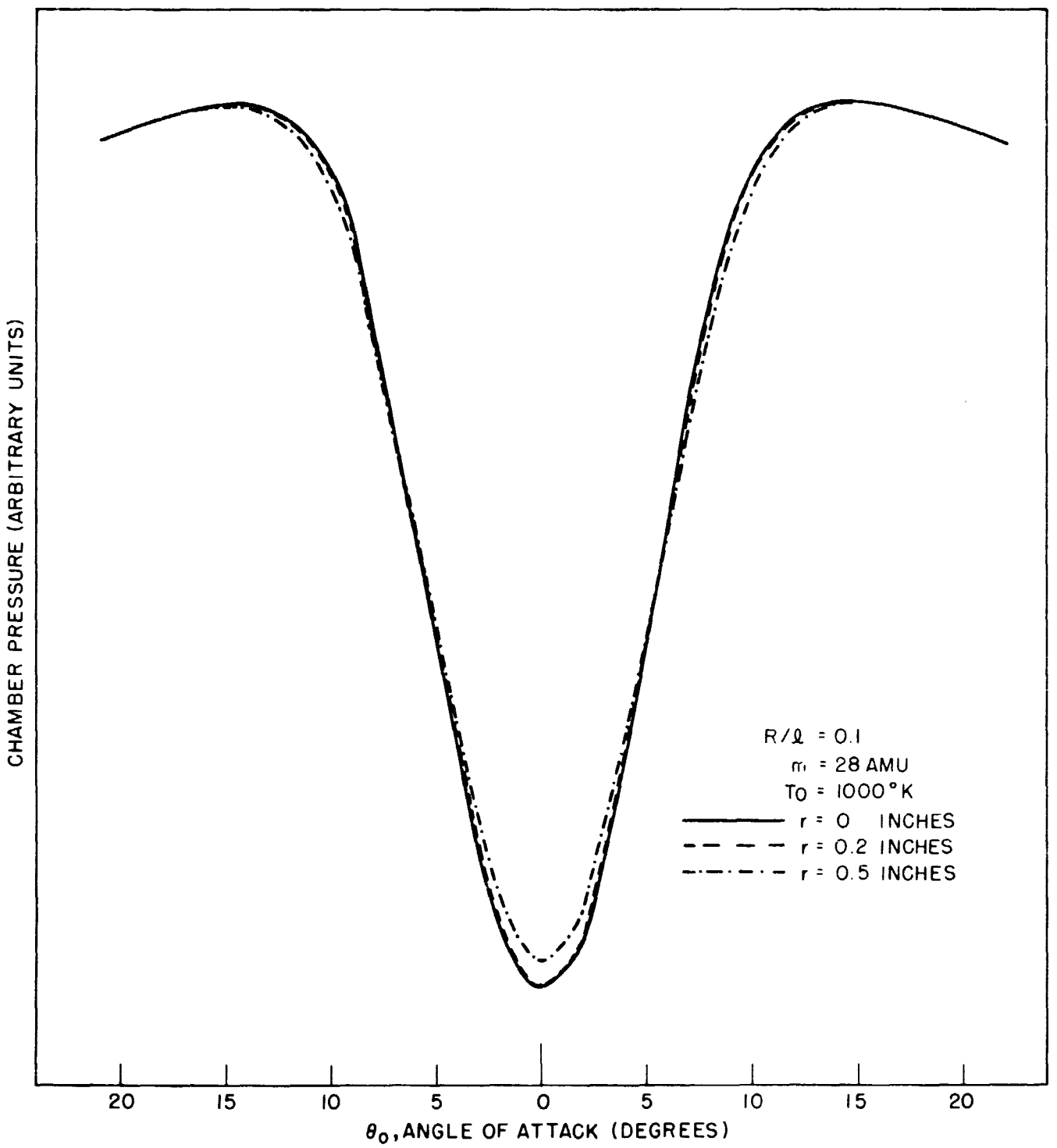

Figure 11—The effect of finite orifice sizes (radius = 0.2 and 0.5 inches) upon the pressure well for $R/\ell = 0.1$ and employing N_2 at 1000° K.

APPENDIX C
The Neutral Wake Experiment on a Non-spinning Spacecraft

In this paper we have limited our discussion to a baffle mounted rigidly in front of an orificed-chamber on a spinning spacecraft. We then rely on the spin motion to scan the wake of the baffle across the orifice. Essentially the same effect can be obtained on a fully stabilized satellite by passing the baffle in front of the orifice in some suitable manner. Depending upon how the baffle movement is achieved, the theory developed here might require little, if any, modification.

One arrangement which offers promise is a propeller type arrangement in which one or more baffles are mounted on a spinning shaft such as shown in figure 12. The advantages of this system are that (1) multiple R/ℓ ratios could be employed to optimize the pressure characteristics for different masses or temperatures and (2) optimum occultation rates can be achieved by selection, or variation, of the drive shaft speed. It would, of course, be necessary to arrange the drive shaft and baffle supports so as to minimize backscattering of particles into the orifice.

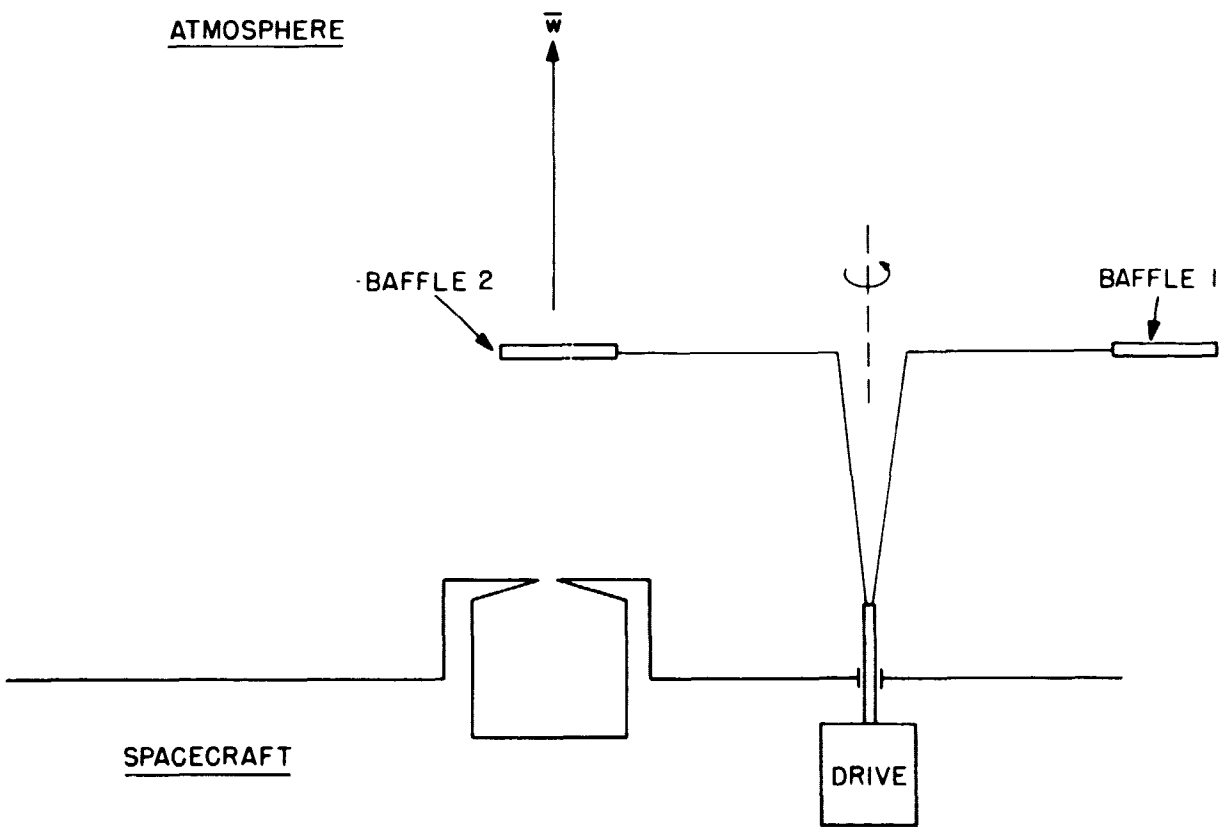

Figure 12–Neutral wake experimental arrangement on a non-spinning spacecraft. Multiple baffles could be used to optimize resolution for various masses and temperatures.